Impact of satellite biases on the position in differential MFMC applications

Steffen Thoelert[1,2], Mihaela-Simona Circiu[1,2], Michael Meurer[1,2]

[1]German Aerospace Center (DLR), Oberpfaffenhofen, 82234 Wessling, Germany
[2]Chair of Navigation, RWTH Aachen University, 52062 Aachen, Germany

ABSTRACT

Global navigation satellite systems (GNSS) are used in many applications and have been part of our daily life since years. In this work error contributions based on the satellite hardware have been investigated and their impact on safety critical applications has been assessed. The paper starts with an introduction of the measurement facility and analysis of the satellite payload imperfections as well as the impact of signal deformations on the pseudo-range for different GPS (Block IIF) and Galileo satellites. The analysis is based on in-phase (I) and quadrature-phase (Q) data captured with a high gain antenna, which offers almost interference and multipath-free signal reception. Using these measurements, the biases for different receiver parameters in terms of correlator spacing and bandwidth are derived. The differential code biases are estimated using a fixed configuration for the ground station, e.g. 0.1 chips for L1 and 1 chip for L5 as specified in the current DFMC MOPS (EUROCAE WG62) and 24 MHz (double-sided) bandwidth. For the user receiver, we extend the receiver parameters to the following design space: 0.01 - 1 chips correlator spacing and 2 – 50 MHz bandwidth for L1, 0.01 – 0.5 chips correlator spacing and 4 – 50 MHz bandwidth for E1, and 0.01 - 1 chips correlator spacing and 10 – 50 MHz bandwidth for and L5/E5a signals. In addition, an analysis of the magnitude of the differential satellite code biases and position errors within the design space defined for GPS L1 (RTCA DO-229E), and within the DFMC design space proposed in the DFMC SBAS MOPS (EUROCAE WG62) is shown. Based on the derived satellite differential code biases, the impact on the position solution for one location and different geometries is presented.

1. INTRODUCTION

Global navigation satellite systems (GNSS) and their applications have been part of our modern life since years. For the transportation of millions of people per year in the air for instance GNSS assisted systems are used like ground based augmentation systems (GBAS), advanced receiver autonomous integrity monitoring (ARAIM) or space based augmentation systems (SBAS) in general. The estimation and modeling of possible error sources is essential to ensure their reliability.

In general, error contributions originate in the satellite payload, the propagation path as well as the user receiver. In this study we focus on the error contribution due to the satellite payload imperfections. These imperfections have been already classified and described as analogue and digital distortions (Mitelman 2004, Phelts et.al. 2009). These distortions yield to biases in the GNSS measurements that affect the position estimation. Satellite biases for various individual satellites and different constellations have been analyzed including their impact on the pseudorange estimation within receivers (Phelts et.al. 2006, Thoelert et.al. 2014).

Based on reference receiver data analysis most of the present safety critical applications try to compensate for typical GNSS errors like clock, orbit, ionosphere as well as satellite biases by the provision of correction values. While the differential applications can mitigate most of the errors that are common between the reference station and the user, one important aspect to consider when analyzing the differential error is that reference and user receiver are not necessarily the same type of a receiver or they might use different configurations for the type of correlator, correlator spacing and input bandwidth. Previous studies showed that the satellite induced biases are different for different receiver types (Hauschild and Montenbruck 2016, Hauschild et.al. 2019). Thus, a remaining bias between the reference receiver and the user (e.g. airborne) receiver is expected after applying the correction values and consequently there is no perfect compensation of the individual errors.

This study will analyze the remaining error contribution of satellite induced biases for single and dual frequency GNSS users considering satellite biases estimated for GPS and Galileo satellites. This output can contribute to any safety critical differential GNSS application to improve their calculation of position solution and the error bounds (e.g. protection levels).

2. FACILITY

For high-quality signal quality analysis, DLR uses a 30m high-gain antenna at ground station Weilheim, Germany (see Figure 1), to capture spectral and I/Q data of GNSS signals. The antenna provides approximately 50 dB gain in the L-band and guide the

signal to a combined L/X-band feed. The feed offers dedicated couplers for various types of polarization and has been configured for right-hand circular polarization (RHCP) signals in the present application.

Figure 1 High gain antenna of DLR at Weilheim ground station, Germany operated by the German Space Operation Center (GSOC)

Behind the feed the signal passes a coupler, low noise amplifier (LNA), filter, and a further LNA. The two LNAs together provide a total amplification of about 70dB, while the filter has a pass-through between 1.1 – 1.65 GHz. After the second LNA, another coupler is installed and finally the signal is input to a vector signal analyzer (VSA) for down-conversion and signal recording. With the VSA it is possible to conduct spectral measurements as well as in-phase and quadrature signal acquisitions with a maximum bandwidth of 120 MHz, a sampling rate up to 326.4 MHz and a recording length of several hundreds of milliseconds depending on the chosen bandwidth and sampling rate. Note that nowadays GNSS signal transmissions are exclusively present with right hand circular polarization (RHCP). The left hand circular polarization (LHCP) capability of the measurement system is only used for validation of the usually very low cross talk characteristic of the satellite antenna. The above mentioned two couplers within the signal chain (before and after the LNAs) offer the possibility to inject calibration signals produced by a signal generator, to provide control on the measurement system behavior. This kind of calibration capability covers the signal chain after the feed. The calibration of the 30 m antenna including the feed is performed using empirical reference data of astronomical sources like Cygnus (Baars et.al. 1966, ITU 2000) and is conducted as described in (Kuz'min 1966, ITU 2000). Detailed information on the overall setup and calibration strategy are provided in Thoelert et.al. (2009, 2013).
The following analysis will benefit from that kind of highly directive antenna by lifting the signal far above the noise floor and avoid incoming environmental distortions from interferences as well as multipath.

3. METHODOLOGY FOR CALCULATING THE RANGE BIASES

Within this work calibrated I and Q data were used as input for the calculation of the range biases at user level based on the satellites signal imperfections. Within the calibration process the above mentioned measurement system calibration information has been applied to compensate for the measurement system impact onto the raw data. Subsequent the troposphere and ionosphere has to be compensated based on weather, respectively space weather information. Furthermore, the Doppler has been removed from the data. Assuming a multipath-free and interference-free data reception based on the narrow beamwidth of the big dish antenna the calibrated data contain only the satellite payload behavior.
Based on the calibrated I and Q data the digital distortions, the power allocation factors of the individual signal components, and the impulse response of the transfer function are estimated in a joint process and can be formulated as

$$\left(\hat{\boldsymbol{\eta}}, \hat{\boldsymbol{\beta}}, \hat{\mathbf{h}}\right) = \operatorname{argmin}_{\boldsymbol{\eta},\boldsymbol{\beta},\boldsymbol{h}}\{\|\tilde{\mathbf{y}} - \mathbf{X}(\boldsymbol{\eta}, \boldsymbol{\beta})\mathbf{h}\|_2^2\}. \quad (1)$$

Where $\tilde{y}$ is the measured signal, β are the power allocation factors, η denotes the digital distortions, h is the impulse response of the transfer function of the satellite, X denotes a convolution matrix, and $\hat{\eta}, \hat{\beta}, \hat{h}$ are the estimates of the digital distortions, power

allocation factors and impulse response, respectively. The method is described in detail in Vergara et.al. (2016) and Thoelert et.al. (2018).
The digital distortions and the impulse response of the transfer function are the input for the estimation of the code range biases. For this analysis the authors follow the approach of Vergara et.al. (2016 and 2019).

4. RECEIVER DESIGN SPACE AND RANGE BIASES

As previously discussed, the satellite code biases are different for different signals and different receiver parameters. In aviation application, the accuracy of the position is improved by the use of corrections computed by the ground stations. In SBAS (Satellite Based Augmentation System), the corrections for each satellite are uploaded to geostationary satellites and are made available to the user. For GBAS (Ground Based Augmentation System), a local differential system, pseudorange corrections for each satellite are broadcast by the ground station directly to the user. When the configuration of the ground receivers and the airborne user are different, the satellite range biases are not completely corrected.
The satellite code biases are computed for all the combination of the receiver configurations with bandwidth between 2 MHz – 50 MHz and correlator spacing from 0.01 to 1 chip (Figure 2a).For E1, the bandwidth was considered 4 – 50 MHz and the correlator spacing 0.01 – 0.5 chips and for L5/E5a 10 – 50 MHz bandwidth . The current airborne specification for GPS L1 (RTCA DO-229E) define allowed regions for configuration of receiver bandwidth and early-minus-late correlator spacing as shown in Figure 2b. For DFMC, the design space has been restricted and is shown in Figure 2c for which the receiver bandwidth can take values between 12 and 24 MHz and the correlator spacing varies from 0.08 chips to 0.12 chips for L1/E5a and 0.8 chips to 1.2 chips for L5/E5a.

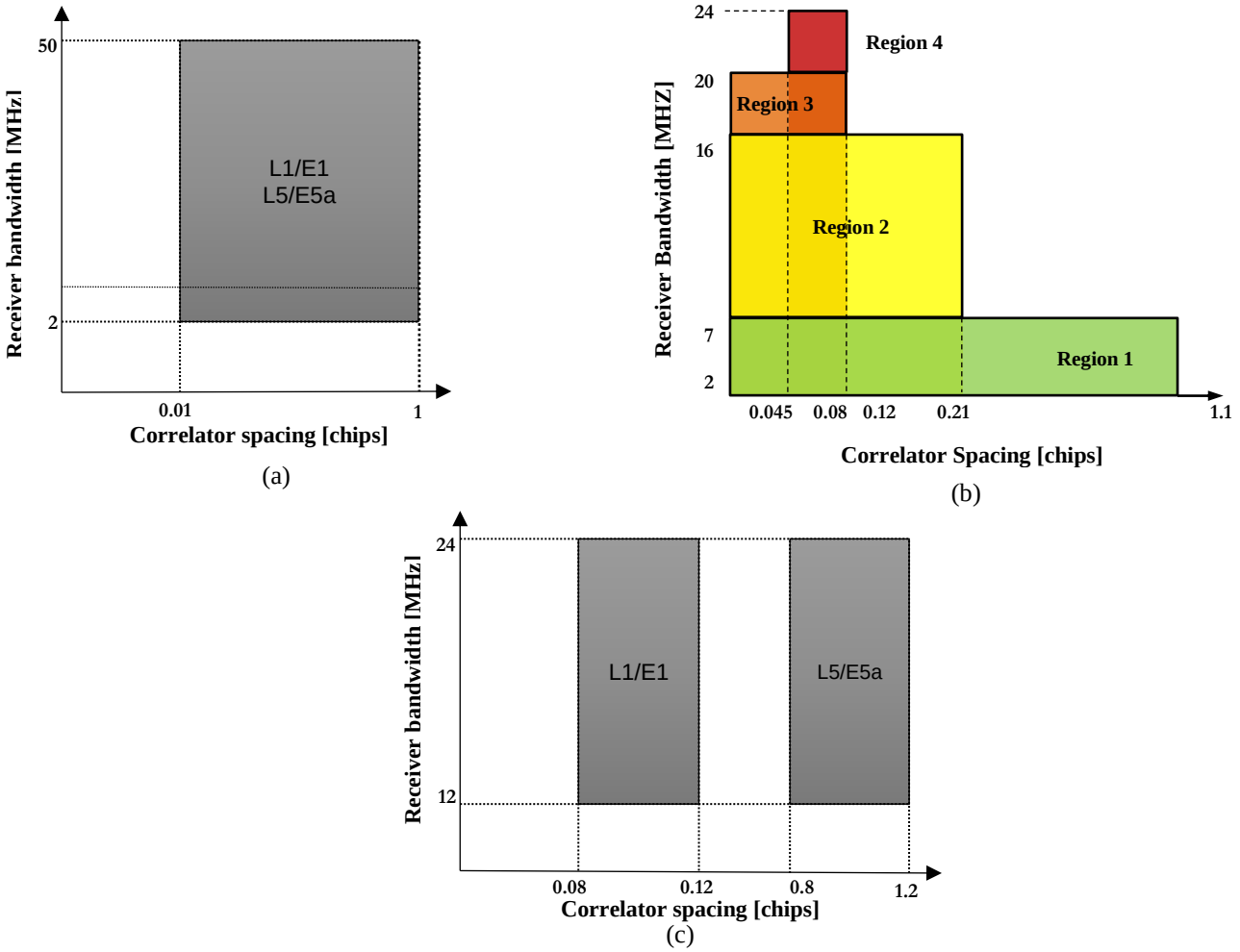

Figure 2 Allowed receiver design space for the entire region considered (a), specified in single frequency GPS L1 standards (b) and for dual-frequency dual-constellation aviation receiver (c)

The differential satellite code biases are computed as the difference between the satellite code bias at the airborne receiver and the satellite code bias at the ground reference receivers and is referred as $\Delta_{bias} = bias_{air} - bias_{gnd}$. In this analysis, the configuration of the ground reference receiver is assumed to be fixed with 24 MHz bandwidth and 0.1 correlator spacing for L1 and 1 chip correlator spacing for L5 (suggested in Mabileau (2018) JWG/3-IP35 as values for SBAS reference stations).

In order to understand the magnitude of these biases, the study starts with the evaluation of the differential satellite code biases for one GPS and one Galileo satellite. The differential code biases are computed for the L1/E1 and L5/E5a band for the entire design space considered in this paper (shown in Figure 2a). For the Galileo E1 signal, the bandwidth minimum bandwidth considered is 4 MHz (as the signal transmitting bandwidth is 4 MHz) and the maximum early-minus-late correlator is set to 0.5 chips. For the L5/E5a signals, the minimum bandwidth is assumed to be 10 MHz.

With the use of a second frequency in the aviation application, a promising processing mode is the ionospheric-free (Ifree) linear combination. The advantage of this processing mode is that it removes the dominant ionospheric errors. However, as the combination makes use of the code measurements from two frequencies, the errors (e.g. multipath and noise error, hardware errors) from both frequencies are combined. This is also applied to the satellite code biases and the total bias affecting the ionospheric-free pseudorange can be described as

$$\Delta bias_{Ifree} = \frac{f_1^2}{f_{L1}^2 - f_{L5}^2}\Delta bias_{L1} - \frac{f_5^2}{f_{L1}^2 - f_{L5}^2}\Delta bias_{L5} \quad (2)$$

The differential satellite code biases present in the Ifree combination will be evaluated as well. For this case, the combinations from the entire design space and the dual-frequency design space are considered. For this analysis, it was assumed that the receiver bandwidth for both frequencies is equal and the correlator spacing on L5 is 10 times larger than the correlator spacing on L1 (which is typically the case for avionics receivers).

Figure 3 shows the satellite differential code biases for GPS PRN 9 for L1 (Figure 3a) for L5 (Figure 3b) and Ifree combination in Figure 3c. It is important to notice that the sign of the differential biases can be negative or positive. For L1, the differential satellite code bias varies from -20 to 60 cm, while for L5 the values range from -20 to 60 cm. The resulting Ifree bias is somewhat smaller varying between -5 to 10 cm. This can be explained by the different signs of the single frequency differential biases, which when combined could compensate each other. Note that this is compensation is not valid for all satellites, as the absolute biases are very different for each signal. The variation within the single frequency design space of the L1 errors remain the same as for the entire space. However, when the dual-frequency space is considered the errors vary in the order of few centimeters for both L1 and L5 case.

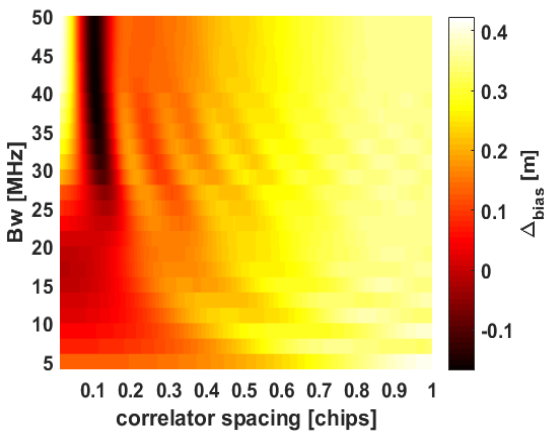

(a)

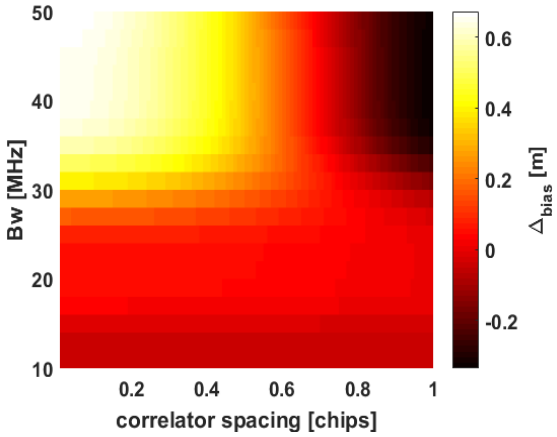

(b)

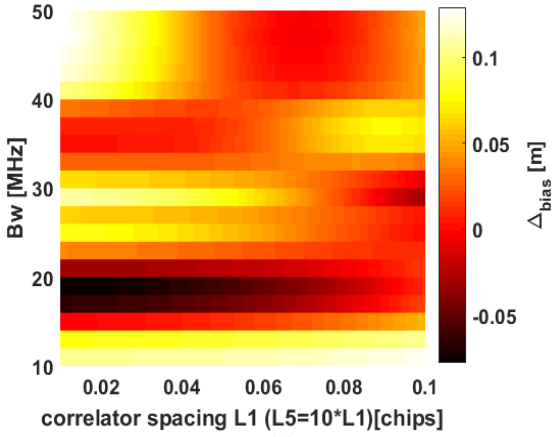

(c)

Figure 3 - Differential satellite code bias for GPS PRN 9 for L1 signal (plot a), L5 signal (b) and Ifree combination (plot c) function of receiver bandwidth and correlator spacing. The ground reference receiver is fixed to BW=24MHz and correlator spacing of 0.1 chip (L1)/1 chip (L5)

In a similar manner, Figure 5 shows the resulting differential biases for a Galileo satellite (PRN 2) function of the receiver bandwidth and the correlator spacing. It can be observed that overall the magnitude of the differential biases is smaller compared with the ones observed in for the GPS example. For E1 signal, the BOC(1,1) replicate is assumed for both receivers and the design space The differential code biases for E1 signals vary from -20 to 35 cm. It can be observed that the biases get larger in the region of 0.2-0.3 chips for all bandwidths which can be explained by influence of the CBOC modulation used on the E1 signal. For E5a, the errors are much smaller varying from -10 to 6 cm. In the Ifree combination, no compensation of the errors occurs in this case and the errors get larger with values between -30 to 30 cm.

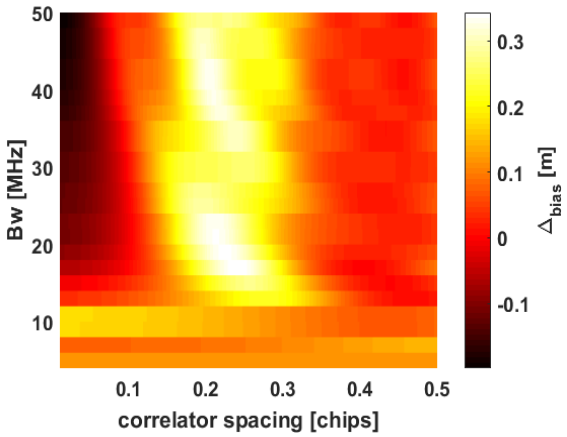

(a)

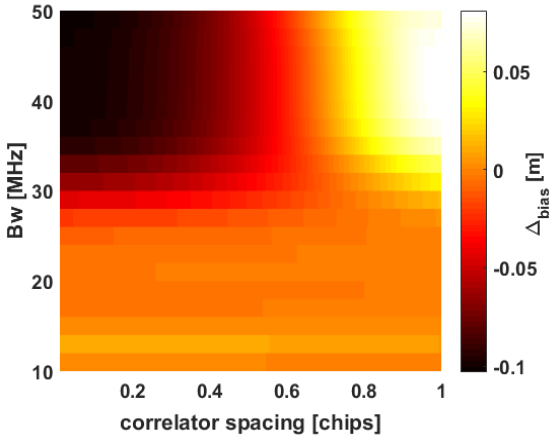

(b)

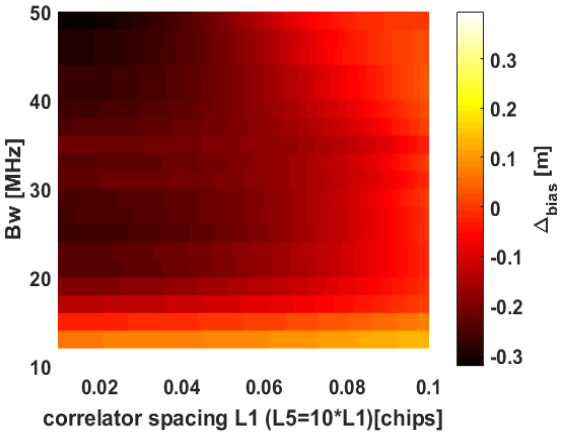

(c)

Figure 4 - Differential satellite code bias for Galileo PRN 2 for E1 signal (plot a), E5a signal (b) and Ifree combination (plot c) function of receiver bandwidth and correlator spacing. The ground reference receiver is fixed to BW=24MHz and correlator spacing of 0.1 chip (E1)/1 chip (E5a)

Based on these results, it becomes clear that the satellite code biases are not negligible. They are different for each satellite and have different signs. Thus they will not be absorbed in the receiver clock estimation, but will yield position errors. In a next step, a study on the impact on the position errors in presented.

5. SIMULATION SETUP FOR POSITION ERRORS

In order to investigate the impact into the position solution, the computed biases are projected into position errors. Different cases are considered such as:

- single-frequency single-constellation GPS L1 position solution
- single-frequency single-constellation Galileo E1 position solution
- single-frequency L1/E1 dual-constellation GPS + Galileo position solution
- single-frequency single-constellation GPS L5 position solution
- single-frequency single-constellation Galileo E5a position solution
- single-frequency L5a/E5a dual-constellation GPS + Galileo position solution
- dual-frequency Ifree single-constellation GPS L1/L5 position solution
- dual-frequency Ifree single-constellation Galileo E1/E5a position solution
- dual-frequency Ifree dual-constellation (GPS + Galileo) position solution

The assumption for the simulations are as follows:

- fixed user location at Braunschweig airport (52°19’9’’N, 10°33’32’’E)
- simulation time: 5 hours from 10:00 – 15:00 (GPS Time). The period was selected such that the maximum number of visible satellite (e.g. 7 GPS Block IIF and 7 Galileo were in view)
- satellites used: 7 GPS Block IIF and 7 Galileo satellites have been characterized for this analysis. In the position solution simulation, only the Block IF satellites were considered and the PRNs of the satellites were selected such that at least 4 satellites are in view during the selected period. For Galileo a complete constellation of 27 satellites was simulated and only the 7 available satellites were used.

The projection into the position solution is performed using the linearized position solution model as

$$\Delta x = (\mathbf{G}^{\mathrm{T}} \cdot \mathbf{G}) \cdot \mathbf{G}^{\mathrm{T}} \cdot \Delta bias_{f,i} \qquad (3)$$

with Δx being the position error vector, $\Delta bias_{f,i}$ the differential satellite code bias (between the user receiver and the reference ground station) for the satellite *i* on frequency *f*, and **G** the geometry matrix. One row of the geometry matrix (for satellite *i*) is described as

$$\boldsymbol{G}_{\mathrm{i}} = [-\cos(El_i)\cos(Az_i) \quad -\cos(El_i)\sin(Az_i) \quad -\sin(El_i) \quad 1\ ], \text{ for single constellation GPS and Galileo solution}$$

The El_i and Az_i represent the elevation and the azimuth angle of the satellite *i.* For dual-constellation, the matrix is built as

$$\boldsymbol{G}_{\mathrm{i}} = [-\cos(El_i)\cos(Az_i) \quad -\cos(El_i)\sin(Az_i) \quad -\sin(El_i) \quad 1 \ \ 0\ ], \text{ for GPS satellites and}$$

$$\boldsymbol{G}_{\mathrm{i}} = [-\cos(El_i)\cos(Az_i) \quad -\cos(El_i)\sin(Az_i) \quad -\sin(El_i) \quad 0\ 1], \text{ Galileo satellites.}$$

The next sections shows and discussed the results obtained for the position errors.

6. RESULTS

For each of the processing mode, the position errors were computed for each single-frequency and dual-frequency mode considering the following three cases for the airborne receiver:

1. the airborne receiver configuration is within the entire design space shown in Figure 2a. For the Galileo E1 signal, the minimum bandwidth considered is 4 MHz (as the signal transmitting bandwidth is 4 MHz) and the maximum early-minus-late correlator space is set to 0.5 chips. For the L5/E5a signals, the minimum bandwidth is set to be 10 MHz;
2. the airborne receiver configuration is within the single frequency design space. This case is only considered for the L1/E1 signals. Also in the case, for E1 the minimum bandwidth was fixed to 4 MHz;
3. the airborne receiver configuration is within the dual-frequency design space (Figure 2c).

The configuration of the ground receiver is considered always fixed to 24 MHz bandwidth and 0.1 chips correlator spacing for L1/E1 and 1 chip correlator spacing for L5/E5a.
During the simulations, the number of satellites varied from 4-7 satellites for both GPS Block IIF and Galileo satellite. The simulated geometries were selected such that they were similar for both constellations, with values of DOP between 1.3 up to 4. Figure 5 shows the skyplot for the GPS Block IIF satellites and the Galileo satellites used in the simulation.

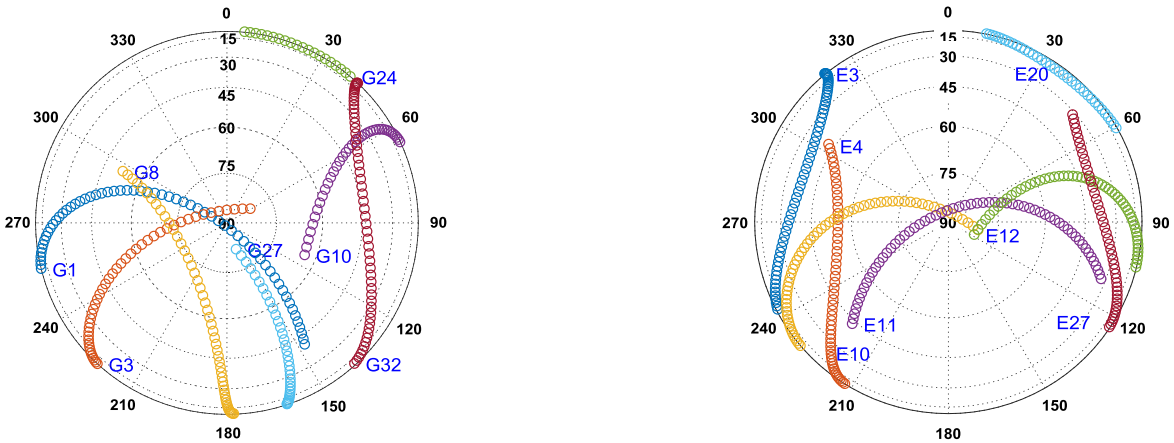

Figure 5 – Skyplot for GPS satellites (left plot) and Galileo satellites (right plot) during the simulation time

For each combination of the receiver bandwidth-correlator spacing, the position errors introduced by the differential satellite biases have been calculated over the simulated time period. The next results show the maximum 3D position error (over the simulated period) obtained for each combination in the considered design space. All the results are shown in a similar manner for all processing modes considered as follows:

- single-frequency single-constellation GPS L1 position solution

Figure 6 shows the maximum 3D errors for the single-frequency single-constellation GPS L1 solution function of the receiver bandwidth and the receiver correlator spacing when the entire design space is considered (Figure 6a), for the single frequency

design space (for the airborne receiver) in Figure 6b and for the dual-frequency design space (Figure 6c). The colors represent the error magnitude and the errors range is the same in all three plots. Looking at the behavior of the errors over the entire design space, it can be observed that they increase with lower bandwidth (lower than 5 MHz) and higher correlator spacing. The errors reach up to 1.4 m for bandwidth larger than 5 MHz and correlator spacing larger than 0.8 chips. When the single frequency design space is considered, the maximum error remains 1.4 m obtained within region 1 (see Figure 2b). Within the dual-frequency design space, the variation of the position errors is much lower and the maximum errors stay below 16 cm.

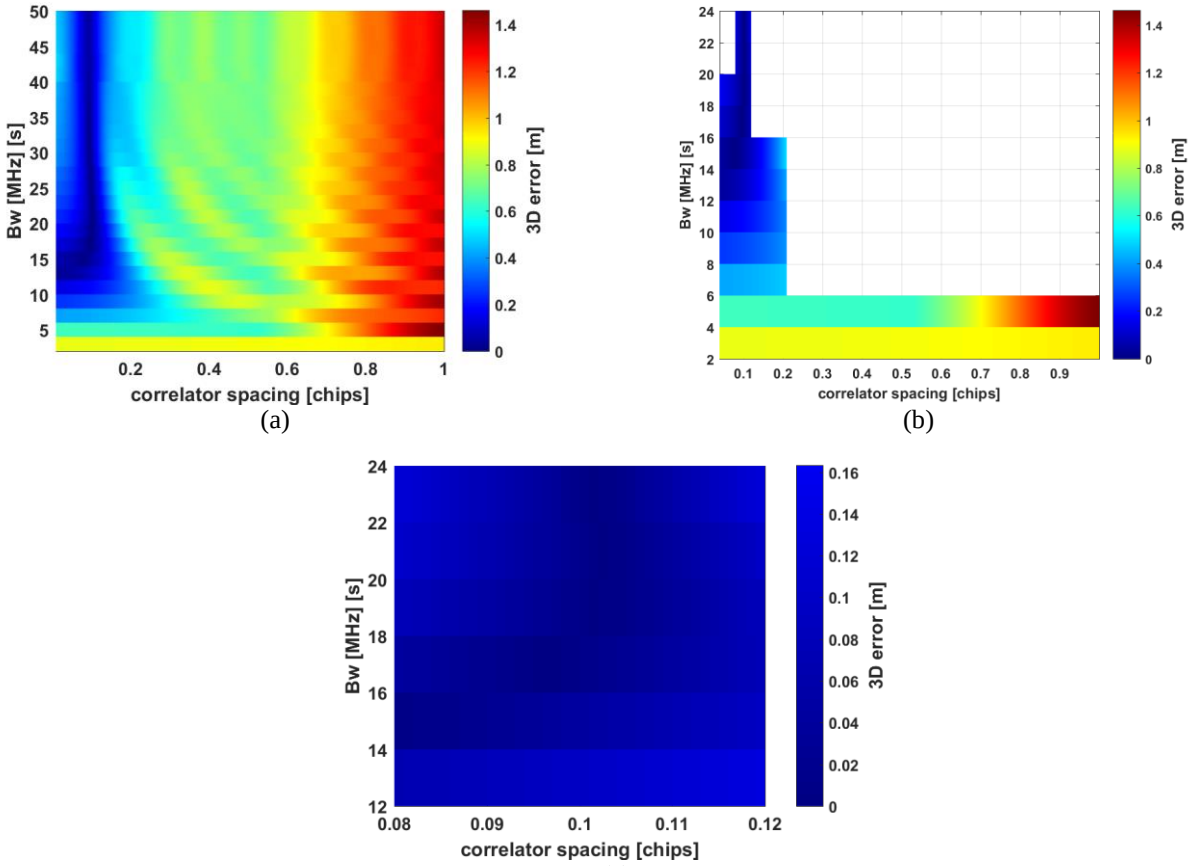

Figure 6 – Maximum 3D error for single-frequency single-constellation GPS L1 position solution for the entire design space (a), single frequency design space (b) and the dual-frequency design space (c)

- single-frequency single-constellation Galileo E1 position solution

For the Galileo E1 case, shown in Figure 7 the behavior of the position error is slightly different. First, it is worth mentioning that the magnitude of the errors is much lower reaching a maximum of 35 cm over the entre design space, 25 cm for the single frequency case and only 3.6 cm for the dual-frequency design space. For bandwidths larger than 12 MHZ, the errors show an increase for correlator spacing around 0.2-0.3 chips. This is explained by the fact that in this region the satellite code biases get larger (see Figure 4) due to small plateaus within the correlation function of the CBOC modulation (Hein et.al. 2006).

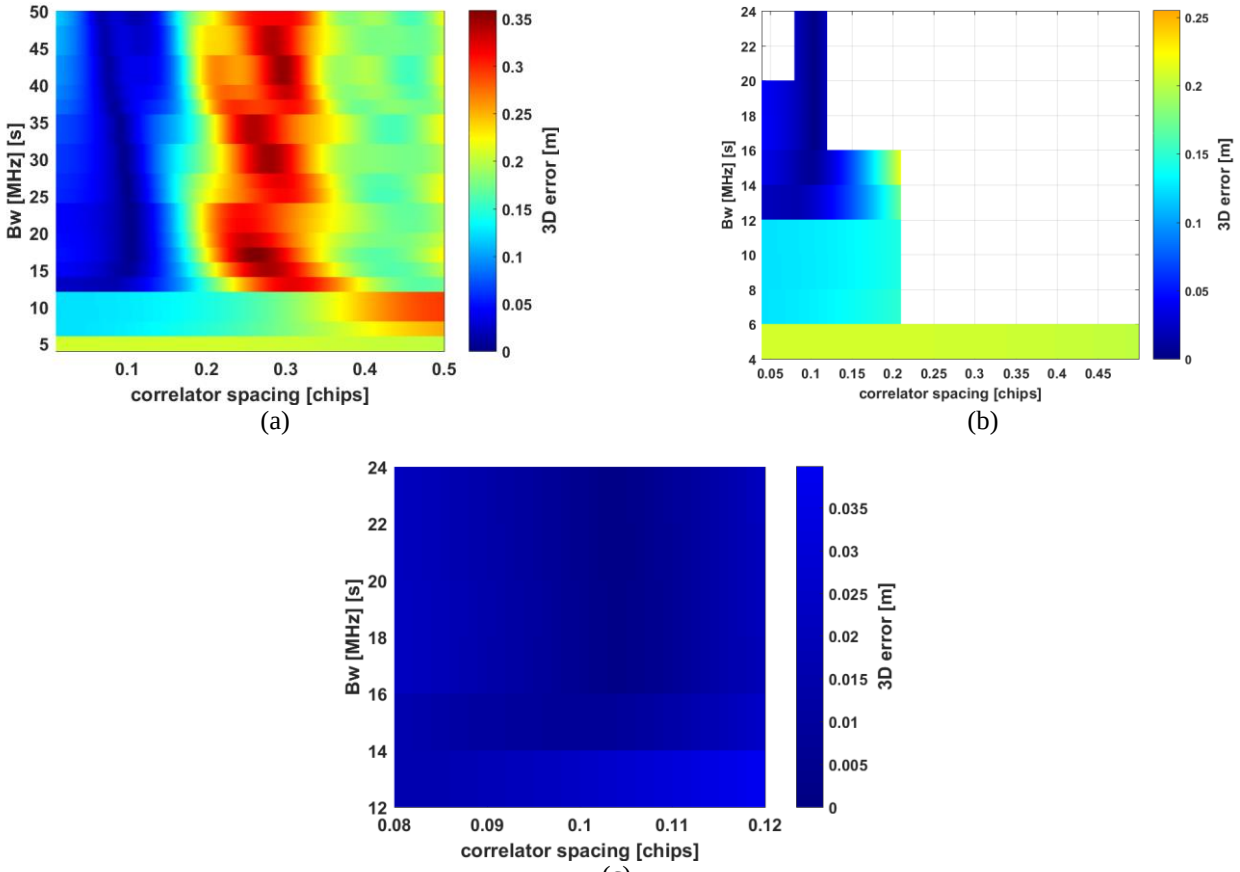

Figure 7 – Maximum 3D error for single-frequency single-constellation Galileo E1 position solution for the entire design space (a), single frequency design space (b) and the dual-frequency design space (c)

- single-frequency L1/E1 dual-constellation GPS + Galileo position solution

When the dual-constellation L1/E1 case is considered, the behavior of the position errors is dominated by the GPS L1 ones and the show a strong increase with the increase of the correlator spacing. This is because the errors obtained for GPS L1 are larger compared with the Galileo E1 ones. The maximum errors obtained reduce to 45 cm for the entire space, 40 cm for the single frequency space and only 8 cm for the dual-frequency design space.

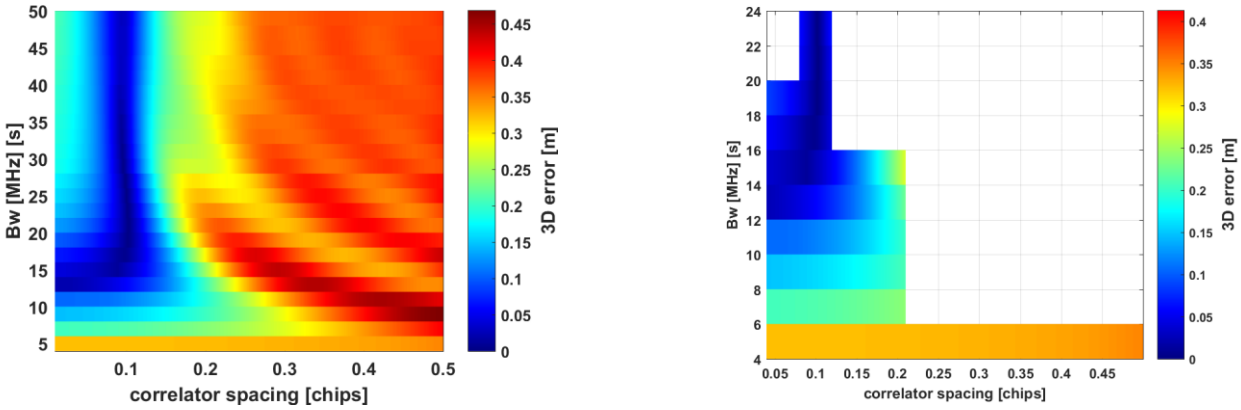

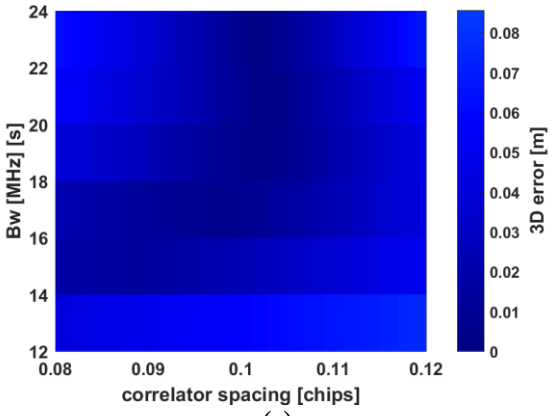

(c)

Figure 8 – Maximum 3D error for single-frequency dual-constellation GPS + Galileo L1/E1 position solution for the entire design space (a), single frequency design space (b) and the dual-frequency design space (c)

- single-frequency single-constellation GPS L5 position solution

The position error obtained for GPS L5 solution are much lower compared with the L1 ones for the entire region and they reach a maximum of 20 cm for wide bandwidth and narrow correlator spacing. The behavior of the errors is opposite from the GPS L1 ones, increasing with the increase of bandwidth and decrease of correlator spacing. This can be attributed to the different modulation on the signal, the BPSK(10). For the dual-frequency region, the maximum position errors stay below 5 cm.

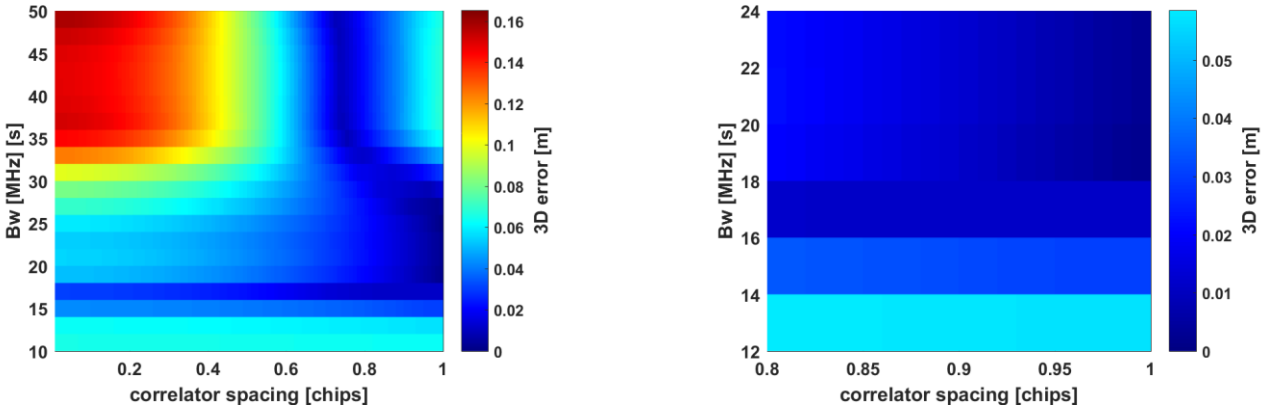

(a) (b)

Figure 9 – Maximum 3D error for single-frequency single-constellation GPS L5 position solution for the entire design space (a) and the dual-frequency design space (b)

- single-frequency single-constellation Galileo E5a position solution

The behavior of the errors obtained for Galileo E5a is very similar with the ones obtained for GPS L5. This is because the two signals have the same modulation, BPSK(10). However, the obtained values are much lower reaching a maximum of 3 cm over the entire design space and only 1cm for the dual-frequency space. The lower errors are due to the lower satellite differential errors for Galileo E5a signals.

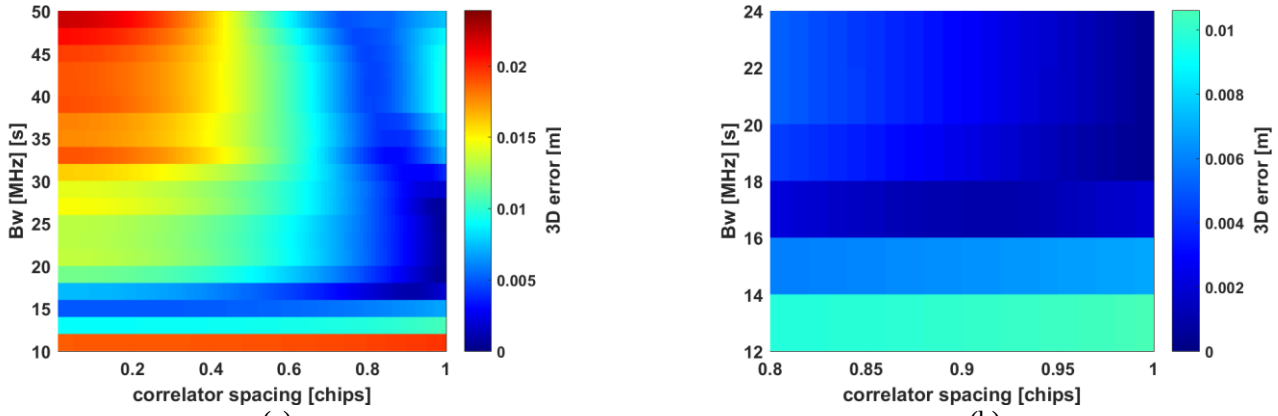

(a) (b)

Figure 10 – Maximum 3D error for single-frequency single-constellation Galileo E5a position solution for the entire design space (a), and the dual-frequency design space (b)

- single-frequency L5a/E5a dual-constellation GPS + Galileo position solution

For the dual-frequency case, the maximum errors obtained are 16 cm for the entire design space and 1 cm for the dual-frequency case. As the errors for both signals have the same behavior, this stays also in the dual-constellation case with error decreasing with wide bandwidth and narrow correlator.

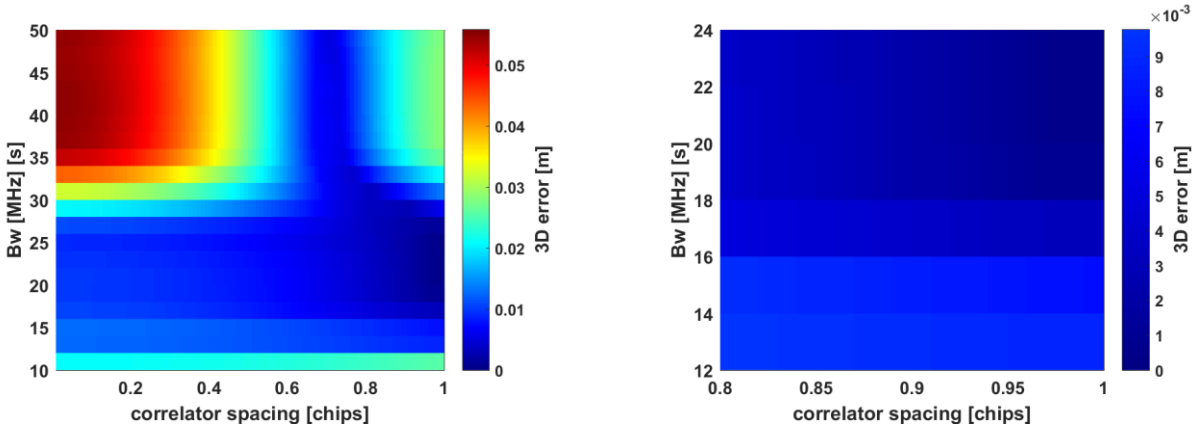

(a) (b)

Figure 11 – Maximum 3D error for single-frequency single-constellation GPS L1 position solution for the entire design space (a), and the dual-frequency design space (b)

- dual-frequency Ifree single-constellation GPS L1/L5 position solution

Figure 12 shows the maximum 3D position errors for the dual-frequency Ifree single constellation GPS L1/L5 mode function of the correlator spacing and receiver bandwidth. The x-axis refers to the correlator spacing for the L1 signal. For L5, the bandwidth was considered the same, and the correlator spacing was assumed to be 10 times larger (in chips) than the L1 one. While this approach might not be the worst case scenario, it is typically implemented in commercial receivers. The behavior of the errors over the entire region is driven by the GPS L5 one, because for narrow correlator spacing (between 0.01 and 0.1) the variation of the L1 errors is rather small. The errors increase thus, with the increase of the bandwidth and narrow correlator and reach up to 1 m.

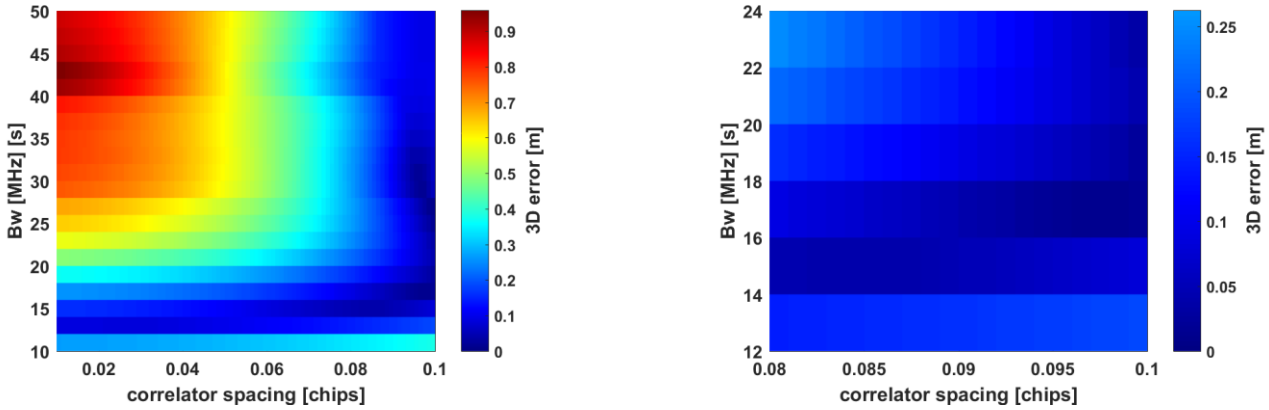

(a) (b)

Figure 12 – Maximum 3D error for Ifree GPS L1-L5 position solution for the entire design space (a), and the dual-frequency design space (b)

- dual-frequency Ifree single-constellation Galileo E1/E5a position solution

Figure 13 shows the resulting error for the Galileo Ifree mode. As the single frequency position errors are smaller for the Galileo signals, also the Ifree combination shows lower 3D errors with a maximum of 30 cm for the entire region and 6 cm for the dual-frequency region.

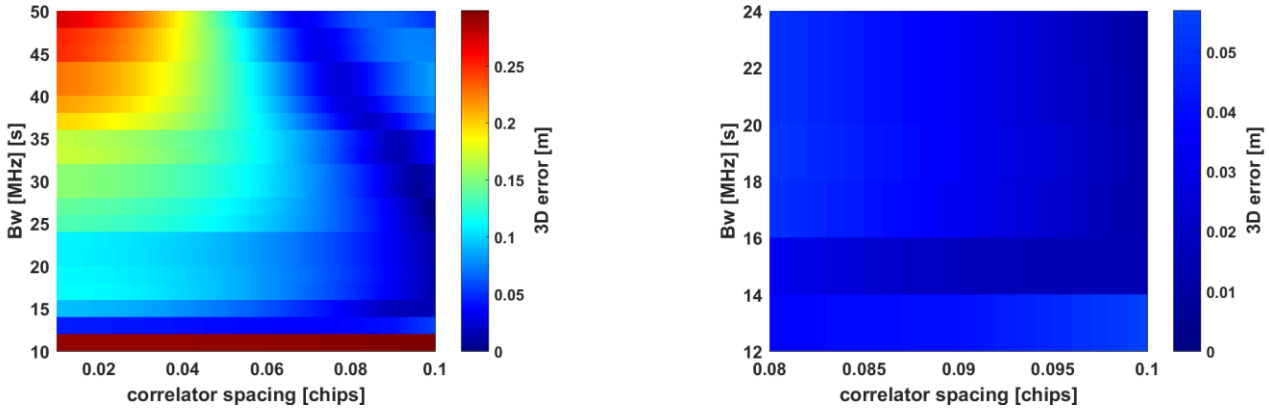

(a) (b)

Figure 13 – Maximum 3D error for Ifree Galileo E1-E5a position solution for the entire design space (a), and the dual-frequency design space (b)

- dual-frequency Ifree dual-constellation GPS L1/L5 + Galileo E1/E5a position solution

In a combined Ifree dual-constellation GPS and Galileo position solution (shown in Figure 14), the error are dominated by the GPS one and increase up to 50 cm over the entire region and up to 15 cm when only the dual-frequency design space is considered.

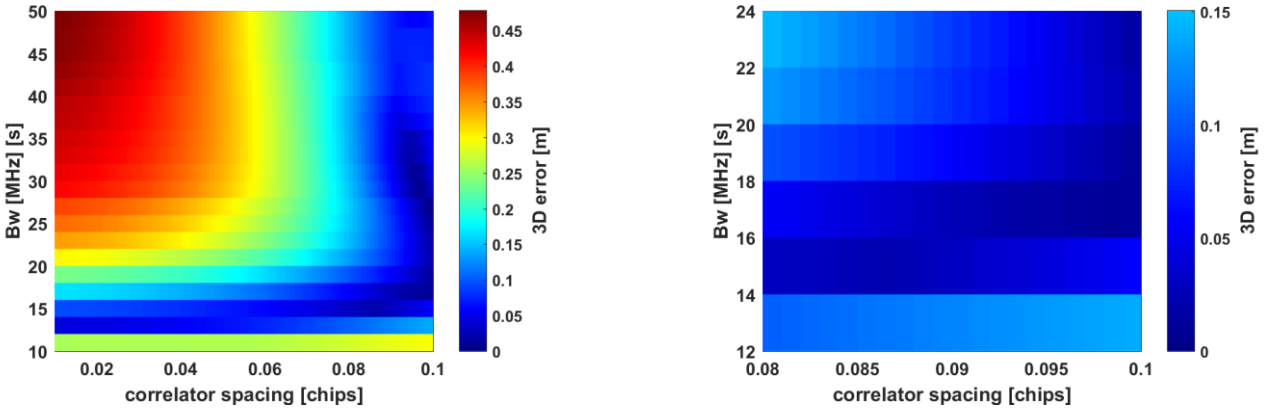

(a) (b)

Figure 14 – Maximum 3D error for Ifree GPS+Galileo L1/E1-L5/E5a position solution for the entire design space (a), and the dual-frequency design space (b)

Table 1 and Table 2 give a summary of the results of the maximum 3D positioning error analysis according the consideration of the entire receiver parameter space and the dual-frequency application space.

Table 1 Maximum 3D position error induced by GNSS satellite biases considering entire parameter space

	GPS [m]	Galileo [m]	GPS + Galileo [m]
L1/E1	1.4	0.35	0.45
L5/E5a	0.16	0.03	0.06
Ifree	1	0.3	0.47

Table 2 Maximum 3D position error induced by GNSS satellite biases considering dual-frequency parameter space

	GPS [m]	Galileo [m]	GPS + Galileo [m]
L1/E1	0.16	0.04	0.09
L5/E5a	0.06	0.01	0.01
Ifree	0.3	0.06	0.15

7. SUMMARY AND CONCLUSION

The analysis of satellite imperfections, satellite induced code biases and consequently errors in the user positioning solution can confirm the presence of satellite imperfections and biases for each GNSS satellite. For the first time the resulting 3D positioning errors have been analyzed considering entire parameter space as well as single- and dual-frequency airborne user design space according correlator spacing and input bandwidth. With a review on the presented results it becomes clear that using a single constellation and according the entire parameter space as well as the single-frequency parameter space the biases have to be taken into account for any user application. The only exception in this case would be a Galileo E5a single-frequency usage. In case of the

dual-frequency use, for both single and dual constellation case, the errors seem to be negligible. But this paper so far only considered 7 GPS and 7 Galileo satellites and therefore a final answer remains open and will be considered in a future publication. On the other hand if the error bound is really tight within a dual-frequency safety critical application the position errors introduced by the satellite code biases have to be taken into account, especially in the Ifree processing.

8. REFERENCES

EUROCAE WG62, Draft Minimum Operational Performance Specification for Galileo / Global Positioning System / Satellite-Based Augmentation System Airborne Equipment, v0.5, November 2017

Hauschild A and Montenbruck O (2016) A study on the dependency of GNSS pseudorange biases on correlator spacing. GPS Solutions, 20 (2), pp 159-171. DOI: 10.1007/s10291-014-0426-0

Hauschild A, Steigenberger P and Montenbruck O (2019) Inter-Receiver GNSS Pseudorange Biases and Their Effect on Clock and DCB Estimation. ION GNSS+, Miami, USA 16.-20. September, 2019

Hein, G. W. et al. "MBOC: The New Optimized Spreading Modulation Recommended for GALILEO L1 OS and GPS L1C." 2006 IEEE/ION Position, Location, And Navigation Symposium (2006): 883-892.

Mabilleau M (2018) "JWG/3-IP35-Galileo evil wave form model methodology," ICAO NSP
- Joint Working Groups, 2018.

Mittelman, Alexander (2004) Signal Quality Monitoring for GPS Augmentation Systems. Doctoral Dissertation, Stanford University, 2004

Phelts RE, Walter T and Enge P (2009) Characterizing Nominal Analog Signal Deformation on GNSS Signals. in Proceedings of the 22nd International Technical Meeting of The Satellite Division of the Institute of Navigation (ITM 2009), Savannah, GA, September 2009.

Phelts RE, Akos DM (2006) Effects of signal deformations on modernized GNSS signals. Journal of Global Position System, Vol. 5

RTCA DO-229E (2016) Minimum Operational Performance Standards for Global Positioning System/Satellite- Based Augmentation System Airborne Equipment. RTCA, 2016

Thoelert S, Vergara M, Sgammini M, Enneking C, Antreich F, Meurer M, Brocard D, and Rodriguez C (2014) Characterization of Nominal Signal Distortions and Impact on Receiver Performance for GPS (IIF) L5 and Galileo (IOV) E1 /E5a Signals. Proceedings of ION GNSS 2014, Tampa, FL, September, 2014

Thoelert S, Hauschild A, Steigenberger P, Langley R and Antreich F (2018) GPS IIR-M L1 Transmit Power Redistribution: Analysis of GNSS Receiver and High-Gain Antenna Data. Navigation, Journal of the Institute of Navigation, 65 (3), page 423-430. Wiley. DOI: https://doi.org/10.1002/navi.250

Vergara M., Sgammini M., Thoelert S., Enneking C., Zhu Y. and Antreich F. (2016) Tracking Error Modeling in Presence of Satellite Imperfections. Navigation - Journal of the Institute of Navigation 63(1):3-13, DOI: 10.1002/navi.129

Vergara M, Antreich F, Enneking C, Sgammini M and Seco-Granados G (2019) A model for assessing the impact of linear and nonlinear distortions on a GNSS receiver. GPS Solutions 24 (5), https://doi.org/10.1007/s10291-019-0917-0